

# Hydrogenase-Coated Carbon Nanotubes for Efficient H<sub>2</sub> Oxidation

M. Asunción Alonso-Lomillo,<sup>†,‡</sup> Olaf Rüdiger,<sup>†</sup> Angel Maroto-Valiente,<sup>†,§</sup>  
Marisela Velez,<sup>||</sup> Inmaculada Rodríguez-Ramos,<sup>†</sup> F. Javier Muñoz,<sup>‡</sup>  
Víctor M. Fernández,<sup>†</sup> and Antonio L. De Lacey<sup>\*,†</sup>

*Instituto de Catálisis, CSIC, C/ Marie Curie 2, 28049 Madrid, Spain, Facultad de Ciencias, UNED, C/ Senda del Rey 9, 28040 Madrid, Spain, Instituto Nicolás Cabrera, Facultad de Ciencias, Universidad Autónoma de Madrid, 28049 Madrid, Spain, and Centro Nacional de Microelectrónica, CSIC, Campus de Bellaterra, 08193 Barcelona, Spain*

Received March 5, 2007; Revised Manuscript Received April 20, 2007

## ABSTRACT

Multiwalled carbon nanotubes grown on gold electrodes manufactured by microtechnology techniques have been used as a platform for oriented and stable immobilization of a Ni–Fe hydrogenase. Microscopic and electrochemical characterization of the system are presented. High-density currents due to H<sub>2</sub> oxidation electrocatalysis, stable for over a month under continuous operational conditions, were measured. The functional properties of this nanostructured hydrogenase electrode are suitable for hydrogen biosensing and biofuel applications.

The unique structural, chemical, and electrical properties of carbon nanotubes combined with the high specificity and sensitivity of biomolecular processes are of great value for biotechnological applications. Controlled immobilization of biomolecules on the high surface area of carbon nanotubes allows miniaturization of biotechnological devices maintaining high transduction signals.<sup>1,2</sup> In particular, direct electron transfer between a redox enzyme (glucose oxidase) and carbon nanotubes has been reported in this way.<sup>3</sup>

Hydrogenases are the enzymes that catalyze in a reversible way the oxidation of H<sub>2</sub> to electrons and protons.<sup>4</sup> The attachment of this type of redox enzymes to electrodes is of great interest as it has potential applications for development of biological water electrolysis or fuel cells<sup>5,6</sup> and electrochemical biosensors<sup>7</sup> that would improve H<sub>2</sub> technology as an energetic alternative to fossil fuels combustion. Several authors have reported direct electron transfer of hydrogenase molecules adsorbed on macroscopic carbon electrodes.<sup>5,8–11</sup> Recently, we have reported a method for covalent immobilization of a hydrogenase with adequate orientation for direct electron transfer toward a highly oriented pyrolytic graphite edge (PGE) electrode that allowed a very stable current due to electroenzymatic oxidation of H<sub>2</sub>.<sup>12</sup>

In this work we report the fabrication of a gold electrode based on microelectronic technologies to which multiwalled carbon nanotubes (MWCNTs) have been grown,<sup>13</sup> electrochemically functionalized, and then covalently modified with hydrogenase molecules in order to obtain a miniaturized biotechnological device that gives high current densities of H<sub>2</sub> oxidation with enhanced stability.

In the first step of manufacturing, thermal oxide (800 nm thick) was grown on 4 in. silicon wafers as an insulating substrate for the electrode fabrication. The metallization was performed in a single process by an electron gun system (Leybold, Unidex 450). A titanium layer (20 nm) and a nickel layer (20 nm) as adhesion promoters followed by a gold layer (150 nm) were deposited as reported before.<sup>14</sup> After fabrication at wafer level, the gold electrodes were separated individually (3.0 mm × 3.0 mm).

The MWCNTs were grown on the electrodes by chemical vapor deposition of acetylene with a floating iron catalyst.<sup>15</sup> The electrodes were placed in the center of a horizontal quartz tube reactor located within a tubular furnace. A mixture of nitrogen, flow rate of 1850 sccm, and hydrogen, flow rate of 40 sccm, was used as carrier gas. The carbon source was acetylene (40 sccm), and the iron catalyst was introduced into the reaction zone by bubbling N<sub>2</sub>, flow rate of 150 sccm, through Fe(CO)<sub>5</sub> maintained at 0 °C (liquid catalyst precursor). The reaction temperature was 750 °C and was maintained constant during the reaction time, 30 min. An average yield of 1.5 mg·cm<sup>-2</sup> of carbon deposited on the electrode surface with an iron content of around 5 wt %

\* Corresponding author: tel, +34-915854928; fax, +34-915854760; e-mail, alopez@icp.csic.es.

<sup>†</sup> Instituto de Catálisis, CSIC.

<sup>‡</sup> Centro Nacional de Microelectrónica, CSIC, Campus de Bellaterra.

<sup>§</sup> Facultad de Ciencias, UNED.

<sup>||</sup> Instituto Nicolás Cabrera, Facultad de Ciencias, Universidad Autónoma de Madrid.

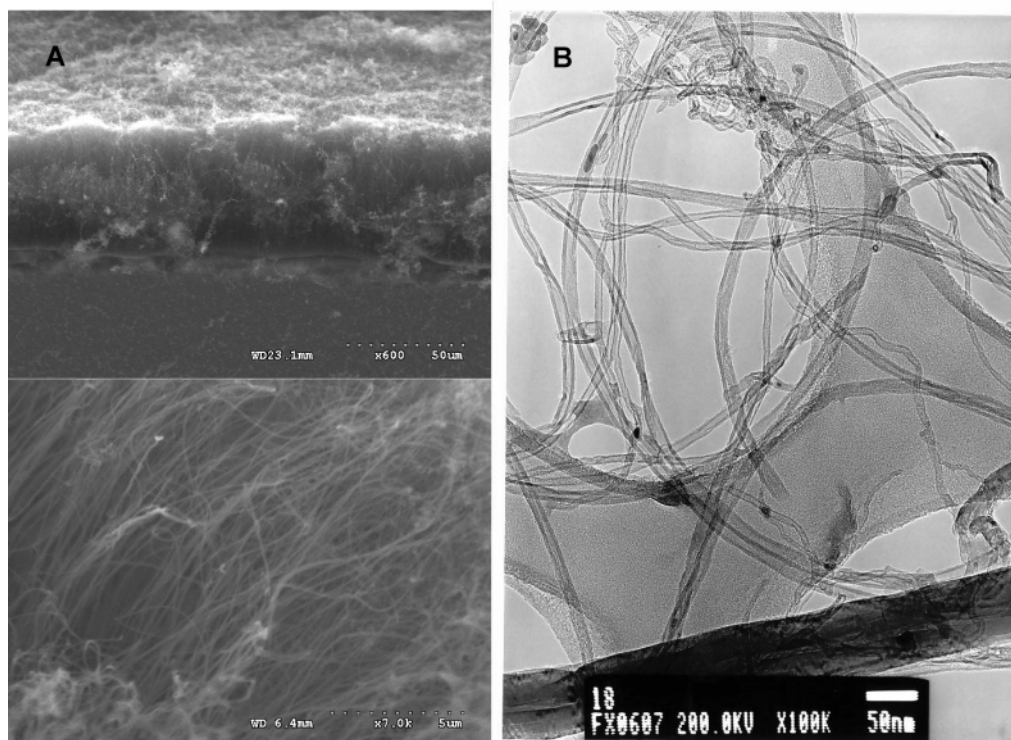


**Figure 1.** SEM (A) and TEM (B) micrographs of synthesized carbon nanotubes.

was obtained. Heating in concentrated HCl of MWCNTs prepared by this method did not decrease the iron content. Therefore, it was concluded that the iron ions are not on the surface of the MWCNTs but encapsulated. Because of this, the harsh acidic treatment was not done for the finally manufactured electrodes described below. The deposited carbonaceous materials were analyzed by scanning electron microscopy (SEM, Hitachi S-3000N) and transmission electron microscopy (TEM, JEOL JEM 2000FX) measurements. The TEM samples were prepared by scratching, grinding, and ultrasonic dispersal in an acetone solution, placed on the copper TEM grid and evaporated.

Figure 1A displays SEM images of the nanotubes grown on the gold electrode surface. The SEM images show a high density of vertically aligned CNTs of an approximate length of 50  $\mu\text{m}$ . The TEM study (Figure 1B) verified the presence of MWCNTs with nonuniform diameters. MWCNTs with average values of outer and inner diameters ranging 15–25 and 5–12 nm, respectively, were observed.

The MWCNT electrodes were surface mounted on TO5 connectors (Vac-Tron S.A., Barcelona, Spain) isolated by an UV-curable polymer encapsulant. The electroactive surface area of the MWNT-modified gold electrode was measured by chronocoulometry of ferrocenemethanol (see Supporting Information). An electroactive area of  $3 \pm 0.2 \text{ cm}^2$  ( $n = 9$ ,  $\alpha = 0.05$ ) was measured for a geometric area of  $0.06 \text{ cm}^2$ , which corresponds to a 50 times increment due to formation of the MWCNT forest. From the TEM images the specific surface area of the MWCNT forest can be estimated as 1000–1500 times the geometric area of the substrate layer, which means that only 2–5% of the area is electroactive. This was expected as the walls of carbon

nanotubes are structurally pyrolytic graphite basal planes; thus only the top of the carbon nanotubes, which corresponds to pyrolytic graphite edge planes, and the defect sites of the walls are electroactive.<sup>16</sup> Functionalization of the MWCNTs was achieved by electrochemical reduction of 4-nitrobenzenediazonium salt in acetonitrile. This method of modification of carbon surfaces was developed by Pinson and co-workers and creates a monolayer of 4-nitrophenyl groups, although polymerization of the aromatic compound on the surface may take place if the conditions of reaction are not carefully controlled.<sup>17</sup> In a second step the nitro groups can be electrochemically reduced to amino groups.<sup>18</sup> Functionalization of carbon nanotubes by electrochemical<sup>19</sup> or chemical<sup>20,21</sup> reduction of aryldiazonium salts has been performed by several authors. In the present work the monolayer of 4-nitrophenyl groups of the MWCNTs electrode was reduced by cyclic voltammetry in 9:1 water/ethanol solution. By integration of the peak area of the cyclic voltammogram, we measured the charge due to the reduction process, which was on average  $0.130 \pm 0.02 \text{ C/cm}^2$  (see Supporting Information). This value is 43 times larger than that obtained upon modification by the same method of a polished PGE electrode, which is in good agreement with the electroactive surface area of the MWCNTs electrode measured by chronocoulometry. This result confirms that only the electroactive surface sites of the MWCNTs electrode are modified by the 4-aminophenyl rings. Covalent immobilization of *Desulfovibrio gigas* hydrogenase to the MWCNT electrode was done by formation of amide bonds between the amino groups of the electrode surface and carboxylic groups exposed on the enzyme surface catalyzed by carbodiimide and *N*-hydroxysuccinimide. We have showed in a previous work

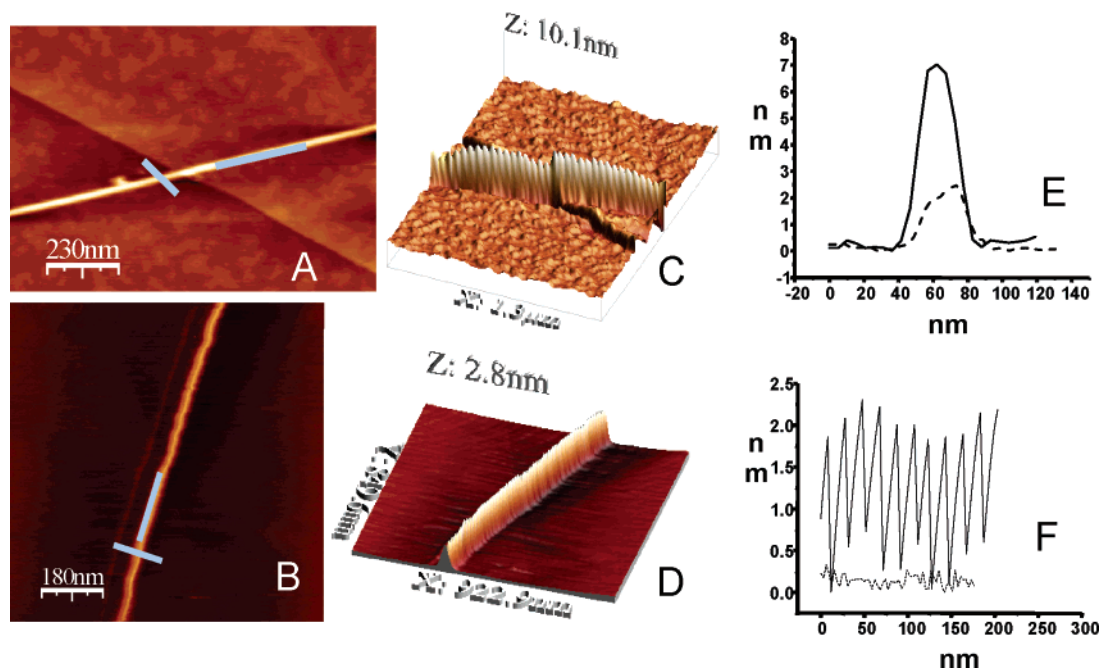


**Figure 2.** AFM characterization of the height and roughness of hydrogenase-coated MWCNTs (panels A and C and solid line in panels E and F) and control MWCNTs (panels B and D and dashed line in panels E and F) deposited on highly oriented pyrolytic graphite.

that under controlled pH and ionic strength conditions this immobilization method allows adequate orientation of hydrogenase molecules attached to a PGE electrode for measuring direct electron transfer between enzyme and electrode.<sup>12</sup>

The hydrogenase-modified MWCNTs were imaged with an atomic force microscope (AFM, Nanotec Electronica, Madrid, Spain). Images were taken in water with the microscope operating in tapping mode. The MWCNTs electrode surfaces were scratched in the presence of water or water with 0.1% Triton in order to solubilize the nanotubes. A droplet of this solution was then put on the surface of freshly cleaved highly oriented pyrolytic graphite. Figure 2 shows that the height and roughness of the protein-modified and nonmodified nanotubes are different. Nanotubes scratched from a protein-modified electrode were more soluble in plain water, indicating that the presence of the protein on the surface had increased their hydrophilic character. The height and roughness difference shown in Figure 2 can be attributed to the presence of a 5 nm thick protein layer covering the modified nanotube, which is in agreement with the three-dimensional structure of *D. gigas* hydrogenase.<sup>22</sup> The difficulty of determining the side structure of the nanotube and the real distance between protein molecules given the limitations imposed by the tip radius does not allow a precise description of the protein density or distribution all along the nanotube surface. However, at least 1 protein molecule every 20 nm in length of the nanotube is present in the thin nanotubes analyzed. The roughness of less hydrophilic and thicker nanotubes solubilized in the presence of 0.1% Triton does not allow distinguishing the individual molecules on their surface. We can then say that in the modified electrodes we are able to clearly distinguish the presence of protein molecules on the

surface of the thinner nanotubes, although we cannot conclude anything reliable about the protein density in nanotubes of increased thickness.

Cyclic voltammetry experiments of hydrogenase-coated MWCNT electrodes shown in Figure 3A indicate that electroenzymatic oxidation of  $H_2$  with very high density current takes place at redox potentials above  $-600$  mV without need of adding a redox mediator for shuttling electrons from the enzyme to the electrode. Previously, a conditioning potential of  $-800$  mV was applied during 90 min under  $H_2$ , in order to obtain full activity of the immobilized hydrogenase.<sup>12</sup>

A sigmoidal shape is observed for the cyclic voltammograms in which the current density above  $-550$  mV almost reached a plateau, whose value increased with the electrode rotation rate. This behavior is indicative of mass transfer of the substrate rate limiting the catalytic process. However, the slope of the quasi-plateau region also increased with the electrode rotation, which suggests that heterogeneous electron transfer between enzyme and electrode started to be rate limiting at the higher electrode rotation rates.<sup>23</sup> The redox process at  $-150$  mV is not related to the catalytic process, and it appears after functionalization of the carbon surface (see Supporting Information). The current densities at  $-0.30$  V of Figure 3A were considered as pseudo-limiting-current densities and fitted quite well to a Koutecky–Levich equation (Figure 3B). The intercept of this plot with the y axis gives the value of the inverse of the current density at this potential in absence of mass-transfer limitations.<sup>9</sup> In this way, a value of  $4.1$  mA/cm<sup>2</sup> at  $-0.3$  V is calculated under those conditions. This value was compared with that obtained with hydrogenase immobilized by the same method on a polished PGE electrode, which was  $0.125$  mA/cm<sup>2</sup> (see Supporting Information). These values are proportional to



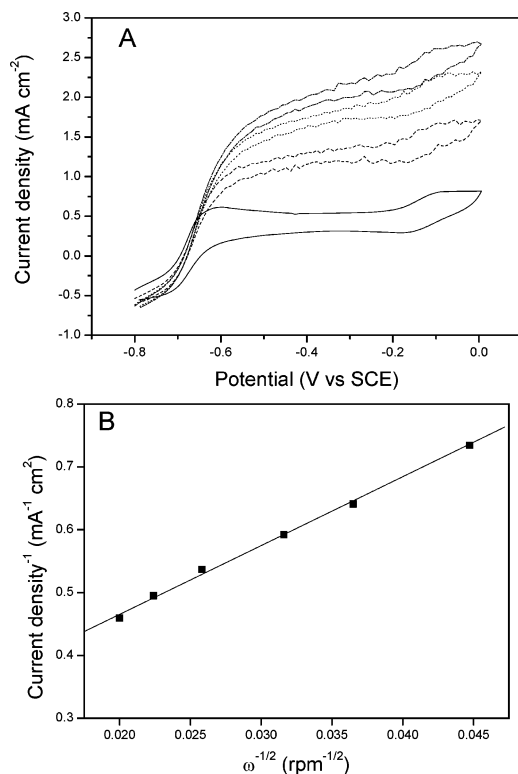


**Figure 3.** (A) Cyclic voltammograms of H<sub>2</sub> oxidation catalysis with a MWCNTs electrode modified with covalently bound hydrogenase. Measurement conditions were 100 mM phosphate buffer, pH 7.0, 40 °C, 1 atm H<sub>2</sub>, 20 mV/s scan rate; 0 rpm (solid line), 500 rpm (dashed line), 1500 rpm (dotted line), and 2500 rpm (dashed-dotted line) electrode rotation rate. (B) Koutecky–Levich plot of current density read at  $-0.3$  V.

the turnover number of the immobilized hydrogenase and to the enzyme coverage on the electrode.<sup>9</sup> As the turnover number should be the same in both cases (the hydrogenase was immobilized by the same method, thus the rate of the limiting step should be also the same), we conclude that immobilization of the hydrogenase on the MWCNTs electrodes gives a coverage of electroactive enzyme 33 times larger than that obtained with the polished PGE electrode. This number is the same order of magnitude as the ratio of amino functional groups generated on the electrode surface (per projected area unit) between both types of electrodes mentioned above. Therefore, almost all the modified surface of the MWCNTs electrode was accessible to hydrogenase immobilization by covalent bonds. This allowed the measurement of density currents at  $-0.3$  V similar to the best results reported by other authors for hydrogenase directly adsorbed onto carbon electrodes, which almost equaled the performance of Pt-based electrodes.<sup>5,24</sup>

At redox potentials below  $-700$  mV negative currents due to H<sub>2</sub> production catalyzed by the bound hydrogenase were also detected. This later catalytic effect is doubled when H<sub>2</sub> is replaced by N<sub>2</sub> (see Supporting Information), which is due to the suppression of the inhibition effect by H<sub>2</sub> on the H<sub>2</sub> production activity of NiFe hydrogenases.<sup>25</sup> It is noteworthy that this inhibition by 1 atm H<sub>2</sub> is much less than that observed in other hydrogenase electrodes, including those manufactured by us with polished PGE electrodes.<sup>12,25,26</sup> We

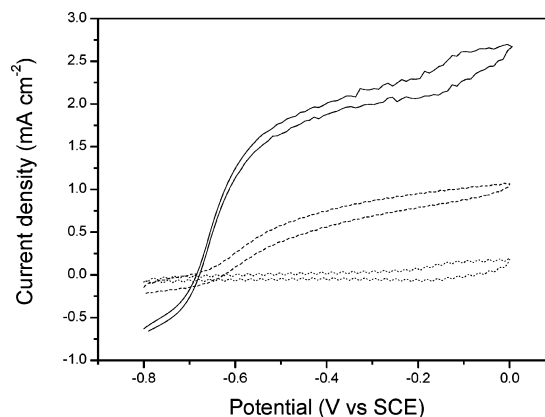


**Figure 4.** Cyclic voltammograms of H<sub>2</sub> oxidation catalysis with MWCNT electrodes modified with hydrogenase by covalent bonds (solid line), adsorption (dashed line), and electrostatic interactions (dotted line). The dotted line also represents the control without hydrogenase. Measurement conditions were 100 mM phosphate buffer, pH 7.0, 40 °C, 20 mV/s scan rate, 2500 rpm electrode rotation rate, 1 atm H<sub>2</sub>.

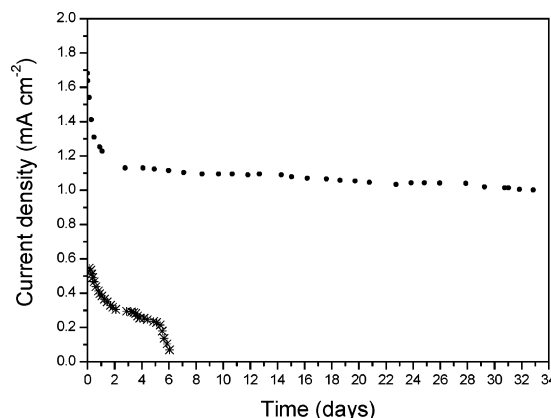


**Figure 5.** Chronoamperogram of H<sub>2</sub> oxidation at  $-520$  mV with MWCNT electrodes modified with covalently bound hydrogenase (●) and adsorbed hydrogenase (\*). Measurement conditions were 100 mM phosphate buffer, pH 7.0, 40 °C, 2500 rpm electrode rotation rate, bubbling of the solution with 1 atm H<sub>2</sub>.

may speculate that this could be due to depletion of H<sub>2</sub> concentration within the forest of MWCNTs.

Control experiments were done in which hydrogenase was directly adsorbed to a MWCNT electrode that had not been modified with the 4-nitrobenzenediazonium salt, or in which no hydrogenase was deposited to the chemically modified MWCNTs, or in which no EDC and NHS were added for the reaction between hydrogenase and the aminophenyl groups of the chemically modified MWCNTs (Figure 4). No catalytic currents of H<sub>2</sub> oxidation or H<sub>2</sub> production were detected in absence of hydrogenase, confirming that catalysis is due to hydrogenase action and not due to Fe ions present in the MWCNTs. The same result was obtained in absence of EDC and NHS. We interpret this result as electrostatic interactions between protonated amino groups of the modified MWCNT and carboxylic residues of the enzyme are not strong enough for immobilization of the hydrogenase during operation (high ionic strength, high electrode rotation rate), although they modulate orientation of the enzyme

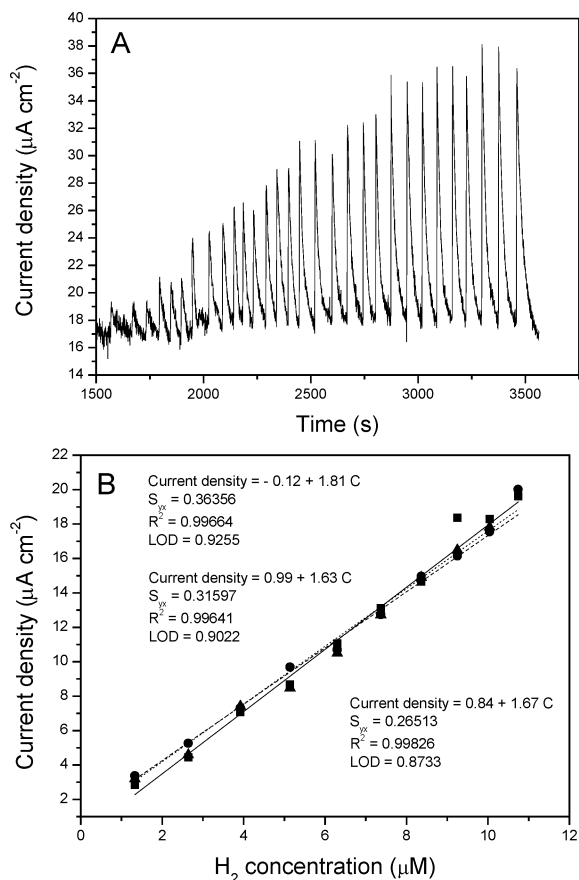


**Figure 6.** (A) Chronoamperogram registered at  $-520$  mV,  $40$  °C, and  $2500$  rpm electrode rotation rate in  $3$  mL of a  $100$  mM phosphate solution pH  $7$ , under  $N_2$  atmosphere. Each addition corresponds to  $5$ ,  $10$ ,  $15$ ,  $20$ ,  $25$ ,  $30$ ,  $35$ ,  $40$ ,  $45$ , and  $50$   $\mu$ L of a  $H_2$ -saturated solution ( $0.8$  mM) by triplicate. (B) Experimental points and linear regressions for three different  $H_2$  calibration curves.

molecules during the immobilization step by covalent bonds.<sup>12</sup> When the hydrogenase was deposited directly on an unmodified MWCNTs electrode, catalytic currents were detected, although considerably lower than those obtained by covalent immobilization. Direct adsorption of hydrogenases on carbon electrodes and their electrocatalytic properties have been described before by several authors.<sup>5,8–11</sup> However, Figure 5 shows that in this case the operational stability of the immobilized hydrogenase was very low; after 6 days there was seldom any catalytic current of  $H_2$  oxidation. On the contrary, the electrodes with hydrogenase immobilized by covalent bonds were very stable. After an initial loss of the catalytic current during the first days, presumably due to desorption of noncovalently bound hydrogenase molecules, there was hardly any decrease after a month of continuous operation.

The performance of the MWCNT electrodes modified with hydrogenase by covalent bonds as a  $H_2$  biosensor was evaluated. The dependence of the response toward the concentration of  $H_2$  in solution was studied by chronoamperometry at  $-520$  mV and  $2500$  rpm electrode rotation rate. Different aliquots of a  $H_2$ -saturated water solution were added to  $3$  mL of a  $100$  mM phosphate solution pH  $7$ , under  $N_2$  atmosphere. After each addition a fast response of the

electrode was obtained, measuring a peak due to an increase in the current density that was quite reproducible (Figure 6A). The average current densities plotted versus the  $H_2$  concentration in the phosphate buffer solution in the range  $1.33$ – $10.74$   $\mu$ M are shown in Figure 6B. The parameters of these calibrations must be optimally evaluated.<sup>27</sup> The existence of anomalous points would lead to incorrect adjustments, altering the sensitivity. In order to avoid this problem, least median squares regression (LMS) was used to detect the existence of these points.<sup>28</sup> Once they were eliminated, a new regression based on the least-squares (OLS) criterion was carried out, in order to obtain optimal precision and accuracy of both slope and intercept. These regressions were used to calculate the limit of detection (LOD) by means of DETARCHI PROGRAM,<sup>29</sup> a program for the calculation of detection limits with evaluation of the probability of false positive ( $\alpha$ ) and negative ( $\beta$ ). The medium LOD was  $0.90 \pm 0.06$  ( $n = 3$ ) with  $\alpha = \beta = 0.05$  and a replicate.

In conclusion, we have shown that a nanostructured carbon electrode formed over gold layers can be used as a platform for oriented and stable immobilization of hydrogenase molecules leading to high-density currents due to  $H_2$  oxidation electrocatalysis. This strategy opens the way for the development of miniaturized  $H_2$  biosensors with high sensitivity and stability and also for the design of small-scale hydrogen biofuel cells. For the later application high-density currents on the anode are compulsory, but also the stability of the electrocatalyst under operational conditions is very important, which is the weak point in most of biological fuels cells reported. In the present work we have made a notable improvement in this aspect.

**Acknowledgment.** We thank Professor Claude Hatchikian for the gift of *Desulfovibrio gigas* hydrogenase and Mr. Ramón Tomé for technical assistance. A.M.V. thanks the MEC in Spain for a contract under the Juan de la Cierva Program. Financial support for this work came from the Spanish Ministerio de Educación y Ciencia (projects CTQ2006-12097 and CTQ-2005-09105-C04-01).

**Supporting Information Available:** Figures of additional electrochemical characterization of hydrogenase electrodes. This material is available free of charge via the Internet at <http://pubs.acs.org>.

## References

- (1) Katz, E.; Willner, I. *ChemPhysChem* **2004**, *5*, 1084.
- (2) Wang, J. *Electroanalysis* **2005**, *17*, 7.
- (3) Patolsky, F.; Weizmann, Y.; Willner, I. *Angew. Chem., Int. Ed.* **2004**, *43*, 2113.
- (4) *Hydrogen as a Fuel: Learning from Nature*; Cammack, R., Frey M., Robson, R., Eds.; Taylor & Francis: London, 2001.
- (5) Karyakin, A. A.; Morozov, S. V.; Karyakina, E. E.; Zorin, N. A.; Pereygin, V. V.; Cosnier, S. *Biochem. Soc. Trans.* **2005**, *33*, 73.
- (6) Vincent, K. A.; Cracknell, J. A.; Clark, J. R.; Ludwig, M.; Lenz, O.; Friedrich, B.; Armstrong, F. A. *Chem. Commun.* **2006**, 5033.
- (7) Lutz, B. J.; Fan, Z. H.; Burgdorf, T.; Friedrich, B. *Anal. Chem.* **2005**, *77*, 4969.
- (8) Butt, J. N.; Filipiak, M.; Hagen, W. R. *Eur. J. Biochem.* **1997**, *245*, 116.

- (9) Pershad, H. R.; Duff, J. L. C.; Heering, H. A.; Duin, E. C.; Albracht, S. P. J.; Armstrong, F. A. *Biochemistry* **1999**, *38*, 8992.
- (10) Lojou, E.; Giudici-Ortoni, M. T.; Bianco, P. J. *Electroanal. Chem.* **2005**, *577*, 79.
- (11) Johnston, W.; Cooney, M. J.; Liaw, B. Y.; Sapra, R.; Adams, M. W. W. *Enzyme Microb. Technol.* **2005**, *36*, 540.
- (12) Rüdiger, O.; Abad, J. M.; Hatchikian, E. C.; Fernandez, V. M.; De Lacey, A. L. *J. Am. Chem. Soc.* **2005**, *127*, 16008.
- (13) Roy, S.; Vedala, H.; Choi, W. *Nanotechnology* **2006**, *17*, S14–S18.
- (14) Alonso-Lomillo, M.; Gonzalo-Ruiz, J.; Muñoz-Pascual, F. *Anal. Chim. Acta* **2005**, *547*, 209.
- (15) Sampedro-Tejedor, P.; Maroto-Valiente, A.; Nevskaya, D. M.; Muñoz, V.; Rodríguez-Ramos, I.; Guerrero-Ruiz, A. *Diamond Relat. Mater.* **2007**, *16*, 542.
- (16) Banks, C. E.; Davies, T. J.; Wildgoose, G. G.; Compton, R. G. *Chem. Commun.* **2005**, 829.
- (17) Pinson, J.; Podvorica, F. *Chem. Soc. Rev.* **2005**, *34*, 429.
- (18) Allongue, P.; Delamar, M.; Desbat, B.; Fagebaume, O.; Hitmi, R.; Pinson, J.; Saveant, J. M. *J. Am. Chem. Soc.* **1997**, *119*, 201.
- (19) Bahr, J. L.; Yang, J.; Kosynkin, D. V.; Bronikowski, M. J.; Smalley, R. E.; Tour, J. M. *J. Am. Chem. Soc.* **2001**, *123*, 6536.
- (20) Heald, C. G. R.; Wildgoose, G. G.; Jiang, L.; Jones, T. G. J.; Compton, R. G. *ChemPhysChem* **2004**, *5*, 1794.
- (21) Lee, C. S.; Baker, S. E.; Marcus, M. S.; Yang, W.; Eriksson, M. A.; Hamers, R. J. *Nano Lett.* **2004**, *4*, 1713.
- (22) Volbeda, A.; Charon, M. H.; Piras, C.; Hatchikian, E. C.; Frey, M.; Fontecilla-Camps, J. C. *Nature* **1995**, *373*, 580.
- (23) Leger, C.; Jones, A. K.; Albracht, S. P. J.; Armstrong, F. A. *J. Phys. Chem. B* **2002**, *106*, 13058.
- (24) Jones, A. K.; Sillery, E.; Albracht, S. P. J.; Armstrong, F. A. *Chem. Commun.* **2002**, 866.
- (25) Leger, C.; Dementin, S.; Bertrand, P.; Rousset, M.; Guigliarelli, B. *J. Am. Chem. Soc.* **2004**, *126*, 12162.
- (26) De Lacey, A. L.; Moiroux, J.; Bourdillon, C. *Eur. J. Biochem.* **2000**, *267*, 6560.
- (27) Alonso-Lomillo, M.; Kauffmann, J.; Arcos-Martinez, M. *Biosens. Bioelectron.* **2003**, *18*, 1165.
- (28) *Robust Regression and Outlier Detection*; Rousseeuw, P. J., Leroy, A. M., Eds.; Wiley: New York, 1989.
- (29) Sarabia, L.; Ortiz, M. C. *TrAC, Trends Anal. Chem.* **1994**, *13*, 1.

NL070519U